

Acoustic emission for detecting deterioration of capacitors under aging

Janusz Smulko¹, Kazimierz Józwiak², Marek Olesz¹, Lech Hasse¹

¹Gdańsk University of Technology, Gdańsk, Poland ²ZPR Miflex S.A., Kutno, Poland

Abstract

There is continuous pressure on production cost reduction of foil-based capacitors, widely used in domestic appliance. Therefore, investigation of the deterioration mechanisms within capacitors is important to reduce their production costs at maintained reliability. These mechanisms were observed in two capacitors batches of classes Y2 (27 nF) and X2 (470 nF). An acoustic emission signal was observed when the capacitors were polarized by excessive voltage. This signal is induced by partial discharges that can lead to capacitor destruction. Next, the capacitors were aged at elevated temperature and also in presence of excessive polarization. We conclude that the acoustic emission signal can predict deterioration of dielectric insulation resistance in capacitors of class Y2. The observed destruction of capacitor of class X2 is caused mainly by detachment of the sprayed metalized contacts that is induced by overheating during partial discharges sparking.

Keywords: capacitor, acoustic emission, partial discharge, reliability

1. Introduction

Foil-based capacitors are popular and ubiquitous elements in electronic power supply units or domestic appliances, mainly to reduce emission of electromagnetic interferences. These elements are quite cheap and can be produced easily but their popularity results in continuous pressure on cutting down their production costs and dimensions. This means that the producers apply cheaper foils and alloys to reduce capacitor size and material costs. Such policy results in sharper demands on controlling their production process. Therefore, the produced capacitors meet the requirements of technical standards but with narrowing margins. Thus, a deeper investigations into their quality and new methods of their reliability prediction are strongly desired because they could help to improve technology at limited production costs and constrained capacitor dimensions.

The main reason of capacitors quality deterioration is associated with partial discharge phenomena that lead to local dielectric overheating and metal layer vaporization during sparking [1]. This process destroys the dielectric in the wound foil and reduces the total capacitance by limiting charge-collection ability within the altered area. Additionally, we can suppose that heat waves affect also other capacitor parts like contacts between the metal cover of the applied dielectric foil and the metal layer sprayed to obtain metalized contacts (Fig. 1). Thus, a more thorough investigation of deterioration mechanisms within the capacitor is necessary to establish the details of their falling reliability.

In this exploratory study, two popular types of capacitors, 470 nF of class X2 and 27 nF of class Y2, made of metalized polypropylene foil were investigated. The requirements and differences between both classes of the capacitors are caused by applying different dielectric thickness and are described in detail in the next section that presents their technology. Two batches of 60 capacitors of each type were experimentally studied. Both types exhibit the ability of self-regeneration, that means local vaporization of the foil metallization and electrical detachment of this region at continuous operation in an electric circuit. This process results in a small decrease of capacitance but does not lead to hazardous short-circuit.

The capacitors were tested by measurement of their standard parameters (capacity, dielectric loss, insulation resistance) and of the acoustic emission signal induced by partial discharges within their structures. Further, the durability test was applied at elevated temperature and in harsh conditions of the supplied intensive voltage pulses. Finally, the capacitors standard parameters were measured again and closing conclusions about their quality and reliability were drawn.

2. Technology of capacitors manufacture and its potential failures

The backed-foil capacitors are produced in five separate stages (Fig. 1) [2–3]. The main component is a one-sided metalized polypropylene foil with a margin without metallization. Two foils are shifted and wound together (Fig. 1a). In the next stage, the wound foils are heated up and shaped by stressing between two parallel planes (Fig. 1b). That process is responsible for creation of the voids within the wound foil due to eventual local gas emission at elevated temperature. Such voids can exist within the dielectric foil around numerous inclusions or at a boarder between metallization layer and dielectric foil. The mentioned inclusions inside dielectric structure are usually formed during polypropylene foil metallization when hot metal is sprayed on the foil and some metal particles can penetrate the foil. Next, the metal layers are sprayed on both heads of the wound foil (Fig. 1c). In the end, the terminals are welded (Fig. 1d) and the foil wad is packed together with a self-extinguishing paste to reach its final form (Fig. 1e). The background voltage for partial discharges creation started from 350 V within the tested capacitors and was lower for class X2 having thinner dielectric foil.

The investigated capacitors, except various capacitance, guarantee different industrial safety. Capacitors of class Y2 assure that in case of their destruction there would be no hazards of electric shock when attached to the shunt resistance. In contrast, capacitors of the class X2 can be applied when their short circuit would cause danger of electric shock for stuff. The different classes are received by applying a dielectric of various thickness. The applied polypropylene foil for the class Y2 is 15 μm thick where for class X2 the thickness is only 7,5 μm . The size of the foil wound was 14.4x8.1x22.5 mm (high, thickness, width) for the capacitance of 470 nF and 10.6x5.9x15 mm for the capacitance of 27 nF. Thus, the class Y2 has to withstand a lightning voltage surge of 5 kV (having standardized impulse wave form of rise and decay times: 1.2 μs /50 μs) when the class X2 needs to withstand twice lower voltage pulse.

The main defects of capacitors are caused by poor quality of the applied materials: dielectric or metal alloys. Various intrusions and heterogeneity in the dielectric lead to air voids or intrusions at various places within the metalized foil [4]. These imperfections can be characterized by high electric

field that results in possible sparking during partial discharging and local overheating [5–7]. Sparking within voids depends on their size, shape and inner atmosphere (e.g.: humidity, additive gases) [8]. Thus, technological parameters during production are crucial for the final capacitors quality.

Another potential area where the capacitors could be destroyed are the joints between the sprayed metalized contacts (Fig. 1c) and the wound foil. Their poor quality results in higher capacitor series resistance and possible overheating within this region. When a capacitor is polarized the total current flows through this region and heats it up locally. Moreover, we can observe partial discharges in this part due to some voids between the metal head and dielectric. The existing sparking elevates temperature there as well.

The local heating of the joints between the metal heads and the dielectric causes stress between these two parts having different thermal expansion coefficients. Thus, the type of applied alloy and dielectric to assure the same level of their thermal expansion is crucial to reach high quality products. Unfortunately, we can still expect some difficulties even with carefully chosen expensive materials due to their different thermal conductivity and some temperature differences caused by strongly localized overheating around voids. These differences result in mechanical stresses that can destroy fragile joints between the sprayed metal layer and the foil heads.

3. Acoustic emission measurements

Partial discharges are a widely used phenomenon for determining the quality of various electrical components like cables, capacitors or transformers [7–12]. There are two main methods of partial discharges characterization and measurements. One method observes the voltage or voltage fluctuations during sparking and demands expensive equipment. This method measures only a tiny part of the sparking current because the majority of this current flows inside the dielectric structure and can not be observed. The second method bases on measurements of ultrasounds (acoustic emission signal) generated during sparking. This acoustic signal can be characterized by its frequency spectrum, intensity and other statistical parameters (e.g. skewness, kurtosis) [9, 13, 14]. Some of these parameters, like frequencies of the main spectral components or kurtosis, do not depend on measurement system (e.g. unavoidable acoustic signal dumping on the boarder between the sensor and capacitor) and can more clearly identify sparkling processes. Additionally, when a few acoustic sensors are applied a place of sparkling can be localized.

An acoustic emission (AE) signal is usually observed in the frequency range of 10÷500 kHz and can be registered by applying popular and commonly available data acquisition boards with an appropriate piezoelectric sensors. A Tektronix TDS5034B multichannel oscilloscope and Vallen Systems GmbH piezoelectric sensor VS45-H with a preamplifier were applied to register acoustic emission signals for further detailed processing. The multichannel system registered:

- an AE signal emitted by the capacitor under test C_T ,
- current pulses that flow through the discharge-free capacitor $C_S=500$ pF and are caused by partial discharges in C_T , measured as a voltage drop across the $R=50$ Ω resistor,

- the voltage at the moment when a partial discharge appeared (attenuated by capacitor voltage divider $C_1=14.9$ pF and $C_2=13$ nF).

The sensor was placed on top of the tested capacitor C_T and held slightly by an elastic band (Fig. 2). The slit between the capacitor C_T and the sensor was filled with the same gel as used during a medical USG check-up. The 27 nF capacitor C_T was tested by applying an alternating voltage of 50 Hz and of 1500 V_{RMS} intensity for a period of 60 s, as is recommended by the obligatory technical standards for the electrical strength test (Fig. 3). The 470 nF capacitor was tested by applying DC voltage of 1180 V within a period of 60 s. The acoustic emission signal was measured after the capacitor shorted through a 390 Ω resistance. The voltage signal across the capacitor was measured by using a P6015A Tektronix probe having a 1:1000 voltage divider.

When the acoustic signal exceeded the threshold value that was set a little bit higher above the system background noise level, the oscilloscope registered the signals. Only some of the tested capacitors exhibited partial discharges. We observed up to 20 events of various intensity but with similar shape, typical for acoustic emission phenomena (Fig. 4a) [8]. The current pulses, observed as a voltage drop U_R across resistor R (Fig. 3) were more noise-corrupted than AE signals (Fig. 4b). The voltage signal during partial discharge was also more disturbed by noise than the acoustic emission signal for the 470 nF capacitors. We registered a sequence of 10000 samples separately for each acoustic emission event at a sampling frequency of 10 MHz. The capacitors exhibited various intensities of the AE signal. Up to 20 separate events within 60 s were registered for several capacitors.

We used statistical parameters (standard deviation and kurtosis [9]) to characterize the registered AE signal as was proposed by Gulski and Kreuger [11]. Standard deviation of random signal x indicates dispersion of the registered samples [11]:

$$\sigma^2 = E[(x - E(x))^2] \quad (1)$$

where operator E denotes averaging. Kurtosis is a measure of the "peakedness" of the probability distribution of the signal x as defined by:

$$\gamma_2 = \frac{E(x - E(x))^4}{\sigma^4} - 3 \quad (2)$$

and is equal zero for normal distribution.

The acoustic signal can be also characterized by its power spectrum, estimated by the Welch method [13]. The power spectrum shows which frequency components dominate in the signal on average but the amplitude of this function can vary between the capacitor samples not only due to various intensity of partial discharges but also due to unpredictable acoustic damping between the sensor and capacitor. Kurtosis does not exhibit such disadvantage. This parameter measures how different from Gaussian distribution is the probability distribution of the observed acoustic signal. We can expect an increase of the kurtosis value when only two or three harmonic components dominate within short intervals of the registered AE signal.

When the spectrograms of the individual acoustic emission transients for the capacitors of both investigated capacitance 27 nF and 470 nF are compared, we can conclude that the use of

thicker dielectric results in generation of an acoustic emission signal with a dominant energy component situated at a lower frequency. The applied *Matlab* function *specgram* computes the windowed discrete-time Fourier transform of a signal using a sliding window (a short-time window that shifts within the registered signal). The module of Fourier transform is called spectrogram and represents signal energy distribution in the joined time-frequency domain. Spectrogram magnitude is represented by greyscale. The spectrogram shows how energy of the signal varies with time and which frequency components are dominant. This method is applied for analysis of nonstationary signals that change its frequency components within time as is observed for acoustic emission signals. The sampled acoustic emission signal was divided into consecutive time intervals of length 256 samples. The Fourier transform was calculated for each sample set. The presented spectrograms (Fig. 5, Fig. 6) are limited to the low frequency range only where the essential differences were observed. The main harmonic component for a 27 nF capacitor is identified around 100 kHz as a dark-grey stripe that is parallel to the time axis across the whole spectrogram (Fig. 5). The dominant component for 470 nF capacitor moves to the higher frequencies, a little bit above 200 kHz and is clearly visible at left half of the spectrogram (Fig. 6). These results correspond to the expectations because the doubled thickness of dielectric for 27 nF capacitors means on the average a twice longer distance during sparking within voids or dielectric discontinuities when compared with 470 nF capacitors.

The applied foil was so thin that the capacitors had a feature of self-regeneration that means ability of local metal layer vaporization in a case of a local shortcut due to some tiny metal intrusions within the foil and disconnection of this capacitor part from further usage (charging/discharging ability). Thus, we can suppose that majority of partial discharges took place during sparking through the foil and eventual foil defects increased opportunities for such sparking. Therefore, a dimension characteristic for sparking is related to the foil thickness and we can expect fastest frequency components for thinner foils. Such effect is observed for acoustic emission signal generated at crack formation during material fatigue or corrosion. Acoustic emission signal depends mainly on cracks size but rather not on size of the tested sample. Thus we could expect frequency doubling of the main acoustic signal component between these two capacitor types as we have just observed. However, this subject needs more deep investigations that are out of scope of this experimental study.

The intensity of the registered AE signal was different between both batches. Kurtosis was much lower for class Y2 (27 nF) than for class X2 (470 nF). This means that the registered AE signal changed faster for class X2 (had harmonic component at higher frequency), as was concluded earlier by comparing spectrograms for both capacitor types (Fig. 5, Fig. 6). Furthermore, the batch of class Y2 exhibited numerous samples without any registered event of an AE signal (Fig. 7a).

4. Durability tests and quality prediction

The industry standards require that the manufactured capacitors should pass a longtime durability test. This examination is performed on a statistical probe of the produced capacitors at an elevated temperature of 100 °C and during a 1000 h long test when the capacitors are polarized by excessive harmonic voltage using a continuously-switched circuit between three stages A, B and C (Fig. 8) that assures repeatable polarization as presented in Fig. 9. This test guarantees conditions for

accelerated capacitor aging and is used to predict their quality and reliability. The capacitance and dielectric loss are measured after the test and compared with the results obtained before the test. When the capacitance drop exceed 10% for more than only a few capacitors within the investigated group, the whole batch is recognized as badly produced and should not be sold on the market.

This procedure is time- and energy-consuming. Additionally, it does not answer the question which samples could fail during harsh exploitation when polarized by a low-quality electric power supply with excessively high harmonic components or short and numerous overvoltage pulses. Therefore, we decided to prolong aging tests over the limit of 1000 h required by industrial norms to establish what kinds of deterioration mechanisms are observed in the capacitors. Additionally, we measured an AE signal that is a supplementary source of information about the presence of voids within capacitors and places of overheating. The intensity of the measured AE signal will be compared with various parameters of capacitors measured after aging to investigate if we can predict their future failure.

In this exploratory study we recognized that both investigated batches withstood the 1000 h aging test even if the majority of the samples exhibited presence of partial discharges when polarized in the way mentioned earlier. The observed dispersed intensity of the AE signal (Fig. 7, Fig. 10) confirmed that the samples had various quality. We observed that aging caused degradation of their parameters (capacitance, insulation resistance, dielectric loss). Thus, we investigated whether the registered AE signal gives any information about future degradation after their harsh aging. The linear correlation coefficient r_{xy} between two random variables x and y was used to estimate if there is any correlation between various parameters of the AE signal and the selected capacitor parameters measured after aging. The coefficient r_{xy} estimated for M pairs of variables x and y is defined by [13]:

$$r_{xy} = \frac{\sum_{m=1}^M (x_m - \bar{x})(y_m - \bar{y})}{\left[\sum_{m=1}^M (x_m - \bar{x})^2 \cdot \sum_{m=1}^M (y_m - \bar{y})^2 \right]^{1/2}} \quad (3)$$

The sample correlation coefficient lies between -1 and +1 and will have a bounding value only when the registered variables x, y exhibit a perfect linear relationship (r_{xy} has nonzero value). This statistical hypothesis can be taken on when the following condition is not satisfied:

$$-z_{\alpha/2} \leq \frac{\sqrt{M-3}}{2} \ln \left(\frac{1+r_{xy}}{1-r_{xy}} \right) < z_{\alpha/2} \quad (4)$$

where z is the standardized normal variable, and α is a level of significance.

We observed that the parameters of AE signal data exhibit correlation only with one parameter of the tested capacitors and for class Y2 only: the insulation resistance measured after their aging. There was no statistically significant correlation between capacitance change or capacitance or dielectric loss after aging and AE signal parameters. The detailed results are presented in Table 1. The gathered data are obtained for the capacitor of 470 nF after 1000 h of the aging test. All samples withstood this harsh test as is required by industrial standards for class X2. The extra next 1000 h aging test destructed numerous samples and therefore we were not able to estimate



correlation after 2000 h aging test for class X2. The batch of class Y2 capacitors, that had twice thicker dielectric than class X2, endured a 2000 h long aging test without any failed capacitor. We observed negative correlation between the insulation resistance and AE signal parameters at the 5% level of significance when the estimated value of z falls outside the acceptance region according to (4) and is bounded by $\pm z_{\alpha/2} = \pm 1,96$ [13]. This result was observed for AE signal kurtosis (Fig. 7) and its power spectrum at some of the selected frequencies where local maxima existed (Fig. 5, Fig. 6, Fig. 10).

Table 1. Standardized normal variable z calculated for correlation coefficient between insulation resistance R_i of the tested capacitors measured after a durability test of length 1000 h (470 nF) or 2000 h (27 nF) and parameters of acoustic emission: kurtosis, power spectral density (PSD) at frequencies $f=19,5$ kHz, $f=97,6$ kHz and $f=293$ kHz.

Parameter\Capacitor type	470 nF (after 1000 h)	27 nF (after 2000 h)
Kurtosis	-0,378	-2,591
PSD at $f=19,5$ kHz	-0,546	-2,835
PSD at $f=97,6$ kHz	-0,0993	-1,388
PSD at $f=293$ kHz	-0,156	-2,929

The above mentioned results of correlation between the AE signal and other capacitors parameters are consistent with reasons of the capacitor failures observed after disassembling the failed capacitors (Fig. 11). The main reason of complete or substantial capacitance drop was a detachment of the metalized heads. Even harsh partial discharges were able to destroy only a part of the wound foil and consequently decreased the capacitance only slightly. We suppose that the detachment process is induced by local foil overheating due to intensive partial discharges and mechanical stress between the wound foil and the metalized head across a narrow boarder line (Fig. 12) . Additionally, partial discharges between the foil edge and the metalized heads lead to tiny metal losses only (Fig. 12) and cannot be considered as the main reason of the observed capacitor failure. Thus, we can suppose that capacitors of class X2 having intensive partial discharges would have shorter life span due to local overheating that induces process of metalized heads detachment. At the same time, a very thin dielectric is often completely destroyed locally when affected by partial discharges. The destroyed dielectric does not influence significantly on correlation between intensity of AE signal induced by partial discharges and resistance isolation of the tested capacitor. That result was observed experimentally for capacitors of class X2 having thin dielectric foil.

5. Conclusions

Partial discharges occur only in some of the tested foil-based capacitors and can be characterized by the concomitant AE signal that gives some additional information about their

quality when compared with measurements of their capacitance or dielectric loss exclusively. Intensity of the AE signal was characterized by its power spectrum at selected frequencies or kurtosis. We conclude that intensive partial discharges are correlated with the observed drop of dielectric insulation resistance observed after aging capacitors of class Y2 having a thicker dielectric foil. Thus, deterioration of insulation resistance can be predicted by AE measurements at least in some capacitor types. In case of class X2 local sparking strongly deteriorates dielectric that is excluded from further charging/discharging ability.

The results of extensive charging/discharging during an aging test of 1000 or even 2000 h shows that partial discharges are indirectly responsible for the capacitors failure. The sparking processes initiate local overheating and can result in detachment of the metalized head and complete capacitor failure. This process depends on the mentioned overheating but also on the quality of junction between the wound foil and the metalized heads. Thus, we can only suppose that partial discharges increase the probability of capacitor failure and can be correlated with their average lifetime. This thesis need further and more detailed experimental study.

To sum up the results, we suppose that it would be interesting to look for a method that would recognize at the same time the quality of the foil roll and the joints between the foil and the metalized heads. A good proposal would be to investigate the AE signal generated during mechanically stressing capacitors when fast depolarizing pulses are applied. These pulses could produce mechanical vibrations not only within the foil roll around their inside voids but within the mentioned joints, specifically at points of their delamination. This is a subject of our further study.

Acknowledgement

This research was financed by the Polish Ministry of Science and Higher Education (2009/2010), project no. N N510 350836.

References

- [1] Y. Qu, G. Wu, X. Zhang, X. Li, W. Shu, Detecting Instrument for DC Partial Discharge within Storage Capacitor. IEEE Int. Symposium on Electrical Insulation, pp. 328–331, 2006.
- [2] A. Morley, D. Campbell, "Electrolytic capacitors—their fabrication and the interpretation of their operational behavior", Radio Electron. Eng., vol. 43, no. 7, pp. 421–429, July 1973.
- [3] WWW page of the capacitor producer CAPACOR: www.capacor.com.
- [4] K. Józwiak, J. Smulko, "Methods of quality characterization of foil-based capacitors", Metrology & Meas. Systems, vol. 15, no. 2, pp. 305–316, 2008.
- [5] G. Kil, J. Song, "Study on a Partial Discharge Test for Low-Voltage Electronic Components", J. of Korean Physical Soc., vol 49, no. 6, pp. 2311–2315, December 2006.
- [6] S. Boggs, A. Pathak, P. Walker, "High frequency attenuation in shielded solid dielectric power cable and implications thereof for PD location", IEEE Electrical Insulation Magazine, vol. 12, no. 1, pp. 9–16, 1996.
- [7] J. Reboul, M. Rouff, R. Carin, "Characterization of dielectric films for power capacitors by space charge technique", IEEE International Symposium on Electrical Insulation, pp. 323–326, 7–10 Apr 2002.
- [8] F.H. Kreuger, E. Gulski, A. Krivda, Classification of partial discharges. IEEE Trans. on Electrical Insulation, vol. 28, no. 6, pp. 917–931, December 1993.
- [9] T. Boczar, "Identification of a specific type of PD from acoustic emission frequency spectra", IEEE Transactions on Dielectrics and Electrical Insulation, vol. 8, no. 4, pp. 598–605, August 2001.
- [10] A. Shigeru, S. Hiroyuki, "Ultrasonic Emission Tactile Sensing", IEEE Control Systems, pp. 61–69, February 1995.
- [11] E. Gulski, F. Kreuger, "Computer-aided analysis of discharge patterns", J. Phys. D: Appl. Phys., vol. 23, pp. 1569–1575, 1990.
- [12] J. Sikula, H. Navarova, B. Koktavy, I. Kosikova, P. Koktavy and P. Vasina, "Acoustic emission and partial discharges in ceramic tiles", Acoustic Emission Testing, TUV Austria, pp. 84–87, Vienna 1999.
- [13] J. Bendat, A. Piersol, Random Data: Analysis & Measurement Procedures, Wiley & Sons, New York, 2000.
- [14] J. Mendel, "Tutorial on Higher-Order Statistics (Spectra) in Signal Processing and System Theory: Theoretical Results and some Application", Proc. of the IEEE, vol. 79, no. 3, pp. 278–305, 1991.



Vitae

Dr Lech Hasse is an Assistant Professor at the Department of Optoelectronics and Electronic Systems, Gdansk University of Technology, G. Narutowicza 11/12, 80-952 Gdansk, Poland. He is a member of the board of the Polish Society of Theoretical and Applied Electrotechnics in Gdansk, a member of the Instrumentation and Measurement Systems Section of the Metrology Committee of the Polish Academy of Science and a member of the IEEE.

Kazimierz Józwiak MSc Eng has graduated from the Faculty of Electrotechnics at Łódź University of Technology, Łódź, Poland. He works at the Miflex company and specializes in capacitors technology and production.

Janusz Smulko PhD DSc is an Assistant Professor at the Department of Optoelectronics and Electronic Systems, Gdansk University of Technology, Poland. He is a member of the board of the Polish Society of Theoretical and Applied Electrotechnics in Gdansk, a member of the Microsystems and Sensors Section of the Metrology Committee of the Polish Academy of Science and a member of the IEEE.

Dr Marek Olesz PhD is a lecturer at the Department of High Voltage and Electrical Apparatus, Faculty of Electrical and Control Engineering, Gdansk University of Technology. He received the MSc. and PhD degrees in 1990 and 1998, respectively, both from the Gdansk University of Technology. His current research interests are focused on diagnostics of insulation material, electrical treeing phenomena and power quality. He is a member of the Polish Society of Theoretical and Applied Electrotechnics.

Captions to figures

Fig. 1. Stages of the capacitor production: a) winding two one-side metalized foils, b) baking and shaping, c) spraying metalized contacts, d) terminal welding, e) final packing.

Fig. 2 Capacitors after final package: 470 nF of class X2 (left) and 27 nF of class Y2 (right).

Fig. 3. Tested capacitor placed under the applied acoustic sensor

Fig. 4. Measurement setup applied for investigation of partial discharges in the tested $C_T=27$ nF capacitors

Fig. 5. Signal observed during a partial discharge event within 27 nF capacitor: a) AE signal, b) voltage drop U_R across the resistor R.

Fig. 6. Spectrogram of the part AE signal presented in Fig. 5a for a 27 nF capacitor.

Fig. 7. Spectrogram of the part AE signal for a 470 nF capacitor.

Fig. 8. Kurtosis of the AE signal observed in the set of tested capacitors of capacitance: a) 27 nF and b) 470 nF.

Fig. 9. Polarization circuit of the tested capacitor C_T during a longtime durability test.

Fig. 10. AC voltage time bundles applied to the capacitor during a longtime durability test; U_N – capacitor nominal voltage (the test applied for class Y2: $1,7 U_N$, for class X2: $1,25 U_N$).

Fig. 11. Measurement results of the tested $C_T=27$ nF capacitors: a) resistance isolation, b) power spectral density of the registered AE signal at 293 kHz.

Fig. 12. Foil of the 470 nF capacitor deteriorated by intensive partial discharges: a) with the melted dielectric and b) its detached brownish metalized heads.

Fig. 13. Microscopically examined 470 nF capacitor: a) deteriorated edge of metalized foil with a slight metal loss, b) identifiable junction of the sprayed metal head and the metalized foil (visible border line along the bottom part).

Figures

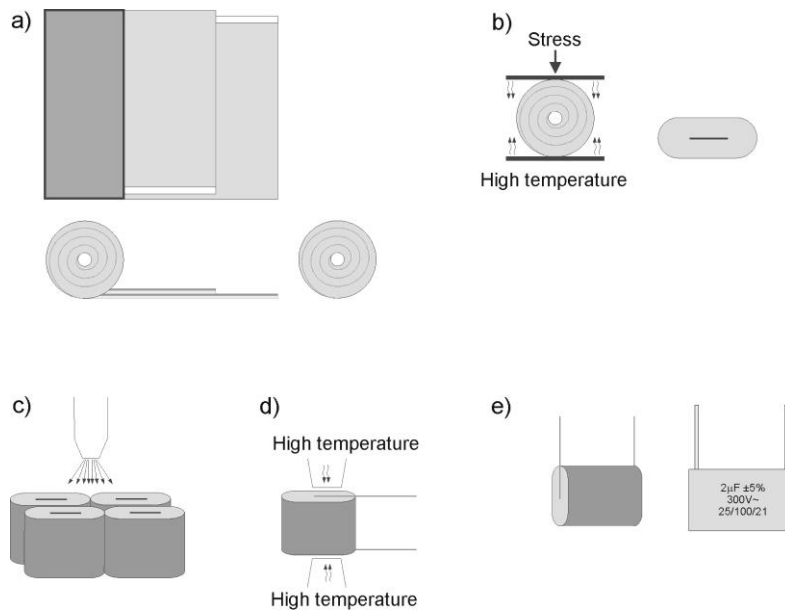


Figure 1

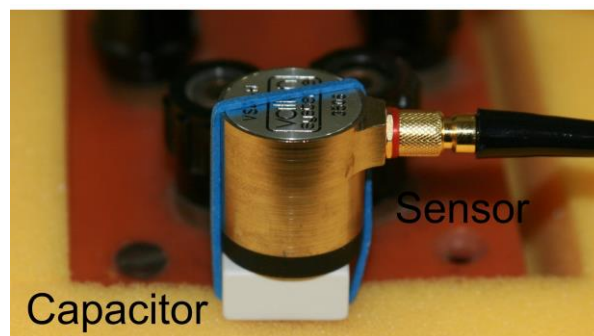


Figure 2

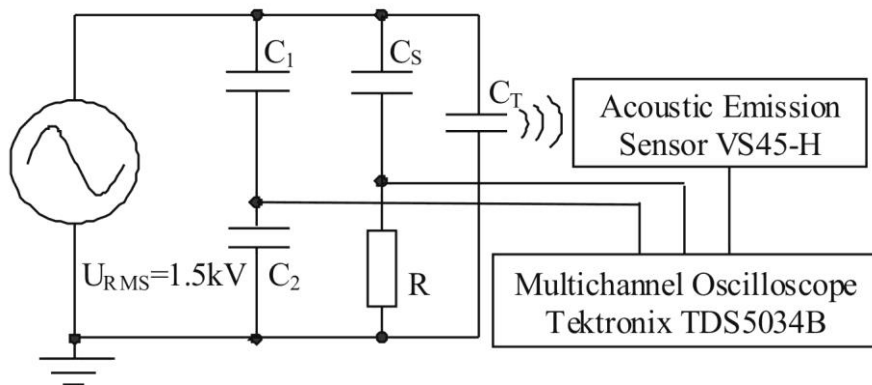


Figure 3

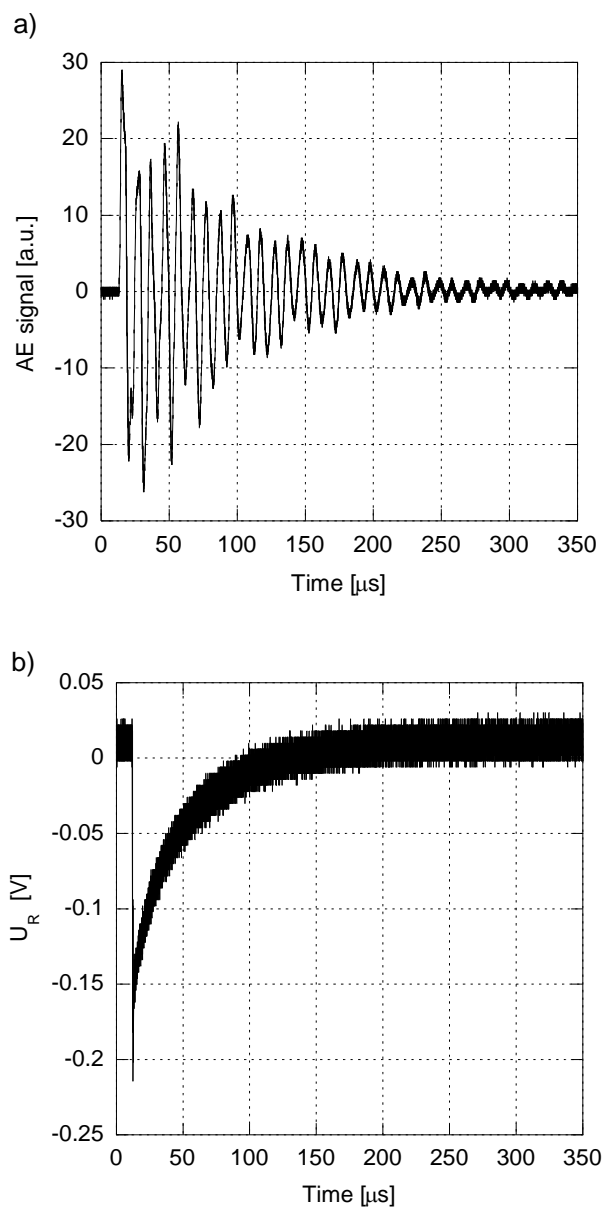


Figure 4

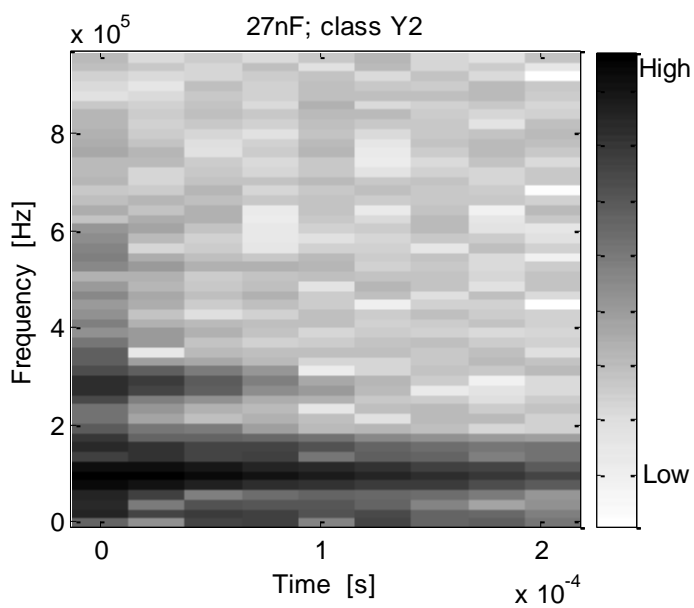


Figure 5

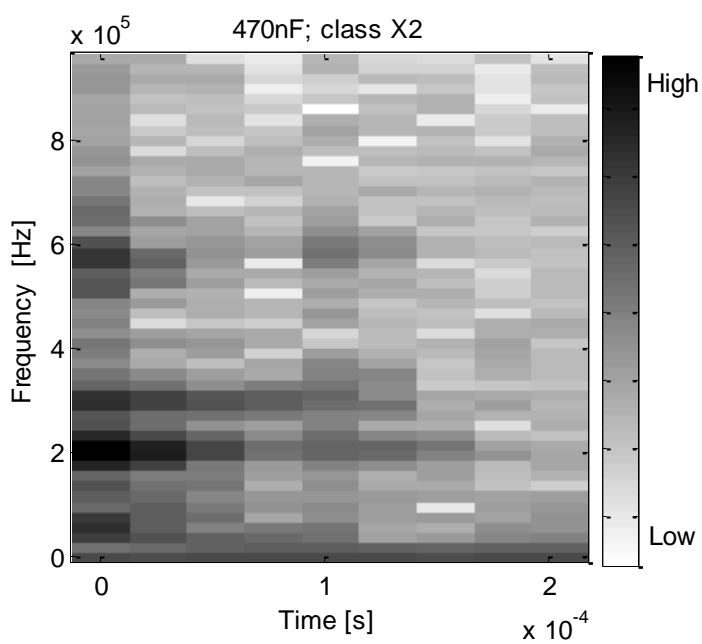


Figure 6



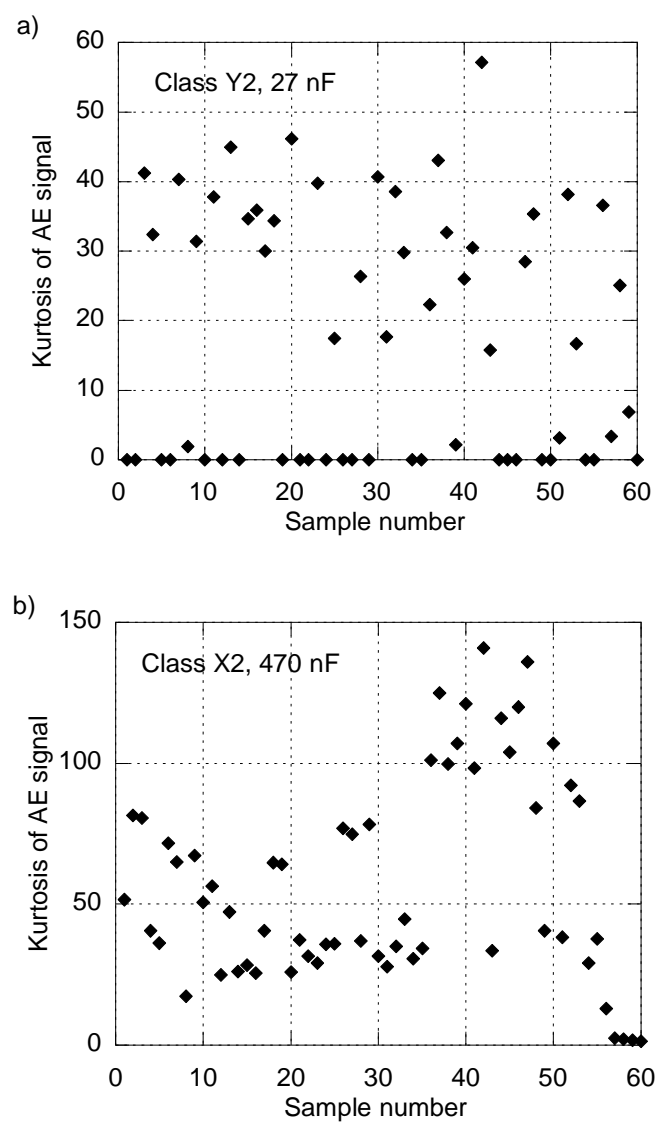


Figure 7

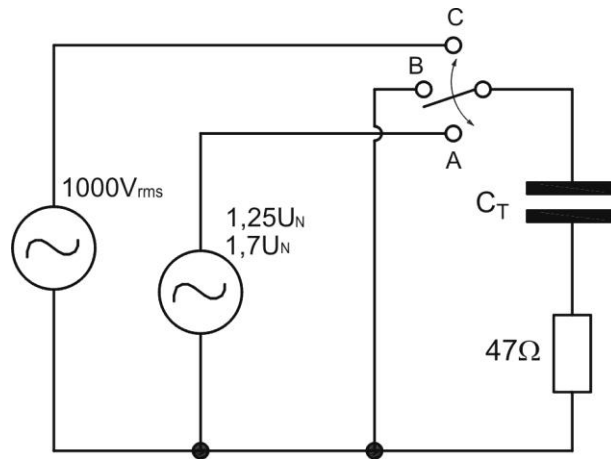


Figure 8

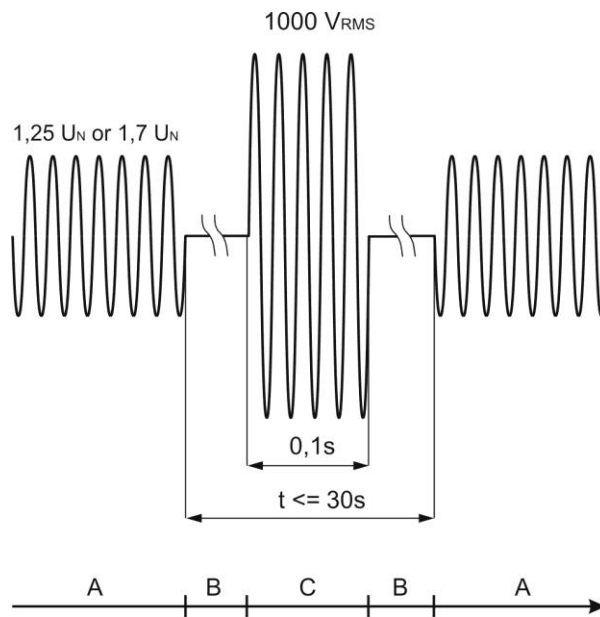


Figure 9

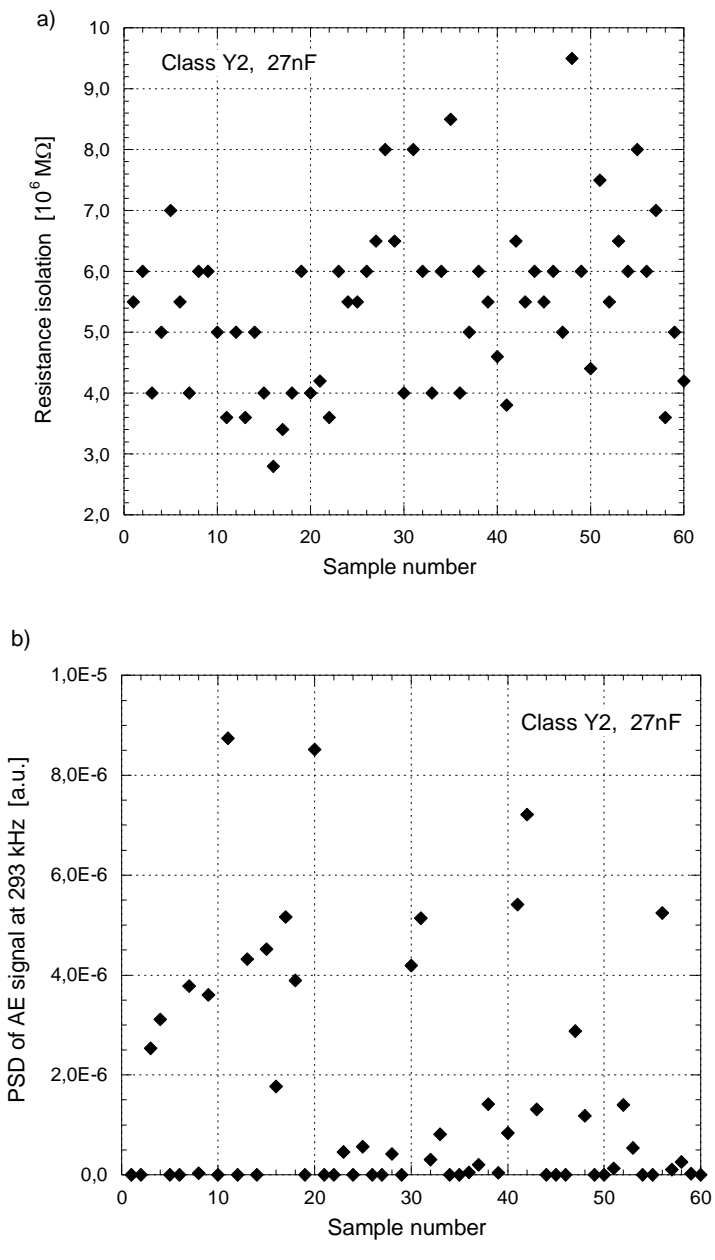


Figure 10



Figure 11

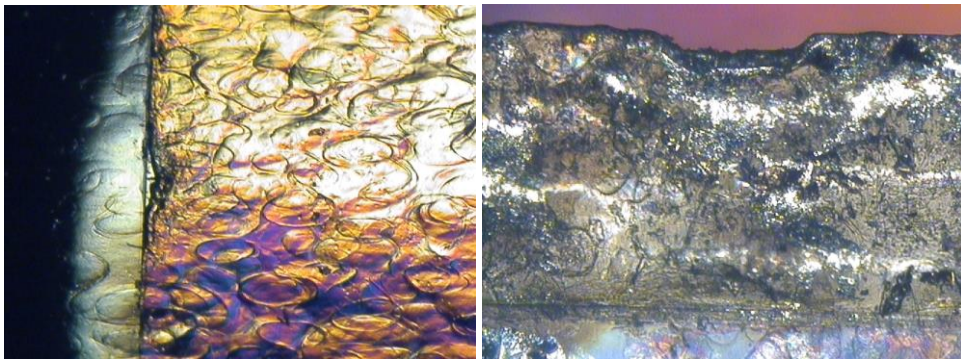


Figure 12